Sensors & Actuators: A. Physical 347 (2022) 113891

Contents lists available at ScienceDirect

Sensors and Actuators: A. Physical

journal homepage: www.journals.elsevier.com/sensors-and-actuators-a-physical

A super high aspect ratio atomic force microscopy probe for accurate topography and surface tension measurement

Xiaolei Ding [a,b,1], Binyu Kuang [c,1], Chun Xiong [c], Renwei Mao [a], Yang Xu [a,b], Zhibin Wang [c,e,f,*], Huan Hu [a,d,**]

[a] ZJUI Institute, International Campus, Zhejiang University, Haining 314400 China
[b] School of Micro-Nano Electronics, Zhejiang University, Hangzhou 310027 China
[c] College of Environmental and Resource Sciences, Zhejiang Provincial Key Laboratory of Organic Pollution Process and Control, Zhejiang University, Hangzhou 310058, China
[d] State Key Laboratory of Fluid Power & Mechatronic Systems, Zhejiang University, Hangzhou 310027 China
[e] ZJU-Hangzhou Global Scientific and Technological Innovation Center, Hangzhou 311200, China
[f] Key Laboratory of Environment Remediation and Ecological Health, Ministry of Education, Zhejiang University, Hangzhou 310058, China

ARTICLE INFO

Keywords:
Ion beam induced deposition
High aspect ratio probes
Tilting angle
Topography scanning
Surface tension
Nanodroplets

ABSTRACT

This work presents a methodology for fabricating high aspect ratio atomic force microscopy (HAR-AFM) probes and its applications in high aspect ratio nanostructure topography and liquid surface tension measurement. The focus ion beam (FIB) precisely positions and grows HAR tips of controlled diameter, height, and tilting angle, which can fabricate robust, repeatable, and multi-angled HAR tips. Through ion beam etching, the probe tip was further sharpened, which helped to achieve a high resolution of topography scanning. We achieved HAR probes fabrication with an aspect ratio of 5–40, a maximum height of 20 μm, a minimum diameter of less than 100 nm, and a tilting angle range of 0–15°. The actual superior performance of FIB-fabricated probes is demonstrated by observing the topography of nano-trenches by HAR AFM probes and compared with commercial pyramid-shaped AFM probes. An additional application is demonstrated that surface tension of micron/nanodroplets could be measured accurately by HAR AFM probes.

1. Introduction

Atomic force microscopy (AFM) probes, as crucial components of AFM, determine significantly the resolution and function of the measurement. An AFM probe consists of a micro-cantilever and a tip at the free end. According to the geometry of the tips of the AFM probes, they can be categorized into pyramid-shaped tips, high aspect ratio (HAR) tips, spherical tips, tipless, etc. HAR AFM probes are increasingly demanded for research of 3-D nanomaterials and nanodevices[1–3] such as FinFET transistors [4–6], biological and molecular materials[7–9], photonic crystals [10–14], etc. Conventional AFM probes have low aspect ratio pyramid or conical tips and are not capable of acquiring accurate topography images since the tip cannot touch the bottom of the deep trenches. On the contrary, HAR probes are more advantageous because they can reach the bottom of these structures with HAR tips and accurately obtain the real topographical information of the structures including bottom morphology and depth[15].

In addition, HAR probes could also be applied in atmospheric science, such as measuring the surface tension of atmospheric particulate matters (PM), which are solid or liquid droplets, with the aerodynamic diameter ranging from around -3 nm to 100 μm. The surface tension of atmospheric PM is important. Because of Kelvin effect [16], the lower the surface tension of PM is, the easier the PM could absorb water and be activated as cloud condensation nuclei, then more cloud condensation nuclei in the atmosphere further impact climate [17]. Surface tension of PM varies because of various chemical compositions in the PM, thus it is important to measure the actual surface tension of PM. The surface tension measurement methods of macroscopic liquids are mature

* Corresponding author at: College of Environmental and Resource Sciences, Zhejiang Provincial Key Laboratory of Organic Pollution Process and Control, Zhejiang University, Hangzhou 310058, China.
** Corresponding author at: ZJUI Institute, International Campus, Zhejiang University, Haining 314400 China.
E-mail addresses: wangzhibin@zju.edu.cn (Z. Wang), huanhu@intl.zju.edu.cn (H. Hu).
[1] Xiaolei and Binyu contributed equally to this work.

https://doi.org/10.1016/j.sna.2022.113891
Received 25 July 2022; Received in revised form 7 September 2022; Accepted 18 September 2022
Available online 20 September 2022

including the pendant drop method [18] and the ring tensiometer [19]. However, although measuring the surface tension of micro/nanometer scale PM is crucial in the study of cloud nuclei formation, there are only limited methods for measuring the surface tension of a single micro/-nanodroplet, including using the HAR probe by AFM [20]. The challenge lies in the difficulty of fabricating nano-scale robust probes of a size suitable for surface tension measurements.

To the best of our knowledge, mainly four categories of methods have been invented to produce HAR AFM tips, and the tips were often long and cylindrical. The first category of the method is to weld or glue a long nanowire to micro-cantilever[9,21–27]. Examples reported include: attaching a single carbon nanotube (CNT) or welding CNTs to AFM probes[9,22]; bonding GaN nanowires to an AFM probe[23]. The GaN nanowires are of higher strength than CNT thus more resistant to bending. The second category of the method is to deposit catalysts on the AFM probe and to grow 1-D nanomaterials in situ[28–30]. For example, Knittel et al. deposited Pt catalysis precisely on the truncated AFM probe tip via focused ion beams (FIB) and then grew silicon nanowires in situ to produce an HAR probe[29]. The third category employed focused electron beams for deposition and focused ion beams for deposition or milling[31–35]. For instance, electron beams were used to induce organic material deposition on AFM tips [35]. The fourth category proposed selective growth of intermetallic silver–gallium nanowires [36–38]. For example, Yazdanpanah et al. described that an Ag-coated AFM probe was positioned over a melted or supercooled liquid drop of Ga between 15 and 25 °C. Then silver-gallium nanowires were co-crystallized[36]. However, most abovementioned approaches lack precise control over the geometry, the tilting angle, as well as the position of the HAR tips. Therefore, methods for fabricating HAR probes with precisely defined geometry, tilting angles and positions are still demanded to ensure high performance, reliability and repeatability.

Here, we demonstrate a methodology to produce HAR probes using FIB-induced deposition. We have optimized the methodology by including the angle control and sharpening the diameter of the HAR probe. We have achieved accurate control of the tip geometry of HAR probes according to the application requirement, with an aspect ratio of 5–40, a tip height up to 20 μm, and a tip diameter from 100 nm to the micron.

2. Experiment

Fig. 1 shows the three major steps of the HAR probe fabrication process. Starting with a commercial AFM probe with a pyramid-shaped tip (Fig. 1(a)), the first step was to employ FIB to remove the top of the tip to render a flat plateau. FIB uses high-energy ion beams to bombard silicon atoms of the silicon sample to achieve the micro/nanometer-scale etching [39,40]. During ion beam etching, the probe was placed vertically on the sidewall of the sample stage, then the sample stage was adjusted to a suitable angle, and an ion beam of 10 pA and 30 kV was selected for etching. The result of the first step was to produce a truncated AFM tip with a diameter of 1 μm for the plateau (Fig. 1(b)). The second step was using FIB to deposit a cylindrical metal platinum column on the flat plateau. The high energy of the ion beam could induce chemical deposition of metallic materials, such as Pt, W and Au, and non-metallic materials, such as C and SiO_2 [41]. In the process of ion beam induced deposition, the AFM probe was placed horizontally on the platform, and the platform was adjusted to a suitable angle for ion beam deposition. In this way, with FIB metal ion deposition, different deposition patterns and deposition parameters can be selected. A cylindrical metal platinum column was selected to be deposited and different parameters were adjusted to obtain a column with an HAR tip of 5–40. Its diameter can range from 100 nm to 500 nm, its height can range from 5 μm to 20 μm and the tilting angle range of the HAR tip was 0–15 degrees (Fig. 1(c)). The tip height was at most around 20 μm due to the limitation of the FIB deposition focusing area, which will be discussed in the Results and Discussion. AFM probe with HAR tip of tilting angle 15° was needed for scanning topography of HAR structure, because after clamping AFM probe to the probe holder in our AFM instrument, there is a tilting angle of ~15°. Therefore, the HAR probe with a tilting angle 15° exactly compensates for this effect [42]. Since the diameter of the obtained cylindrical HAR probe in this step was large, but smaller probe tip diameter was needed. Therefore, the last step was using FIB etching to sharpen the cylindrical tip to obtain a smaller diameter. After FIB etching, the diameter of the cylindrical tip can reach 100 nm or less (Fig. 1(d)). All the steps of this method were ion beam etching and ion beam induced material deposition, which could accurately control the tip geometry including the diameter, height, and tilting angle.

The source of the pyramid-shaped commercial probe was AC160 purchased from Oxford Instruments. The length of the cantilever was 160 μm, and the width was 40 μm. The FIB used in this study (ZEISS crossbeam 350) combined the excellent imaging and analysis performance of the high-resolution field emission scanning electron microscope (FE-SEM) and the excellent processing capabilities of the focused ion beam.

3. Results and discussions

FIB was used to fabricate HAR probes with a maximum aspect ratio of up to 40. Before fabricating the HAR probe, the method was tested for producing HAR platinum nanopillars on a silicon wafer with different heights, diameters, and shapes. Fig. 2(a) are SEM images of nanopillars with increased heights produced by increased deposition durations. The probe was with the largest HAR of about 40, and the maximum height of the nanopillar was about 20 μm. These consistently fabricated probes have much larger aspect ratios than the probes produced by existing methods roughly ranging from 5 to 20. Fig. 2(b) demonstrated that the diameter of nanopillars increases with increased deposition durations. The diameter of the nanocolumn can be controlled stably between 100 nm and 1 μm by controlling the beam irradiation area. This larger range of heights and diameters expands the use of HAR probes for a wider range of application structures, such as abovementioned the FinFET transistors, the biological and molecular materials, and the

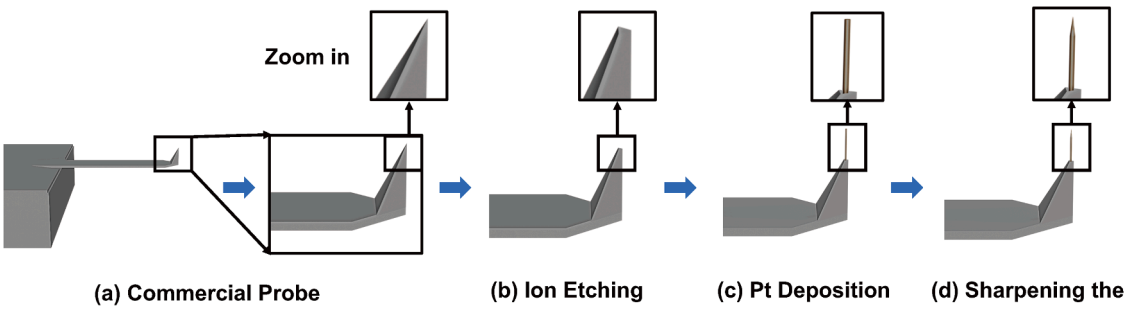

Fig. 1. The fabrication process of a HAR probe using FIB. (a) Commercial AFM probe; (b) Ion beam etching; (c) Ion beam induced Pt deposition; (d) Ion beam etching to sharpen the HAR tip.

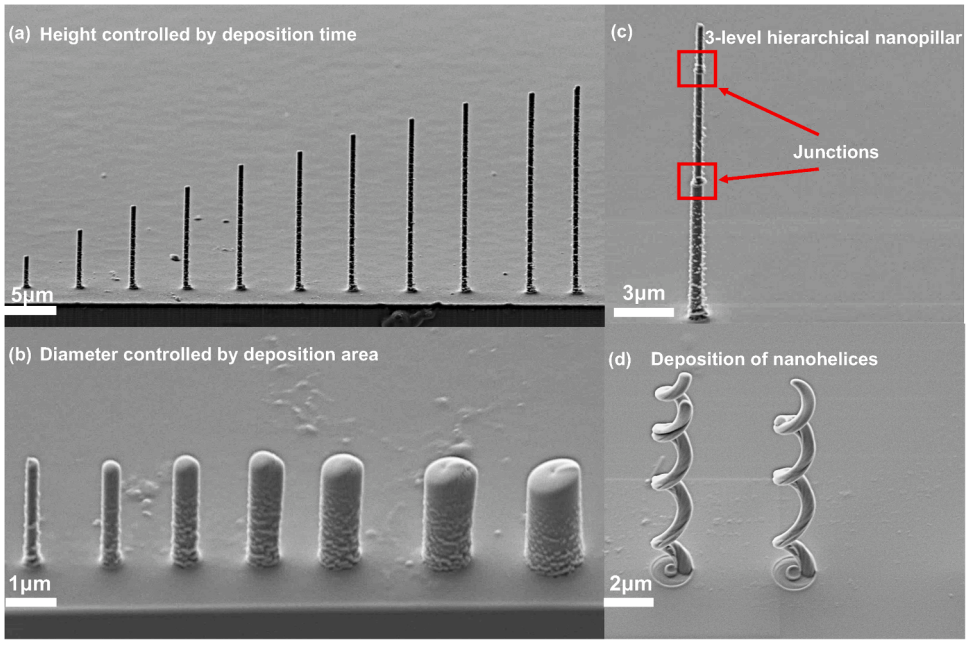

Fig. 2. An SEM image of different nanopillars. (a) Different heights of nanopillars with deposition duration increasing, (b) Different diameters of nanopillars with deposition durations increasing. (c) A 3-level hierarchical nanopillar with repeated deposition, (d) Deposition of nanohelices.

testing of surface tension of microscopic droplets.

However, the growth of the nanopillars cannot increase indefinitely along with increasing deposition durations. As can be observed from Fig. 2(a) that with the increase of deposition duration, the growth rate of the height of the nanopillars slowed down. In order to investigate the reason for the inability to deposit nanopillars indefinitely, we changed the starting deposition point several times. As shown in Fig. 2(c), by depositing a nanopillar first and then depositing another nanopillar atop, higher nanopillars can be achieved. Fig. 2(c) showed a three-level hierarchical nanopillar. This indicates that the height of a single deposition is limited while changing the starting deposition point allows for continuous deposition of nanopillars to increase the height. The reason for not being able to deposit consistently (Fig. 2(a)) may be limited by the FIB deposition focusing area. Within the focusing area of the high-energy Ga ion beam, auxiliary gas containing Pt compounds is adsorbed on the substrate, then reacts with the high-energy Ga ion beam to deposit Pt atoms. With the increasing height of the deposited pillar, the amount of auxiliary gas adsorbed to the top of the pillar is reduced, and more auxiliary gas is evacuated by the vacuum pump, thus only part of the high-energy ion beam was converted to the deposited platinum atoms, while the other part of the energy acted on the substrate, producing sputtered atoms, causing the pillar to be etched and ultimately slowed down the deposition rate.

Fig. 2(d) shows Pt nanohelices produced by FIB demonstrating the

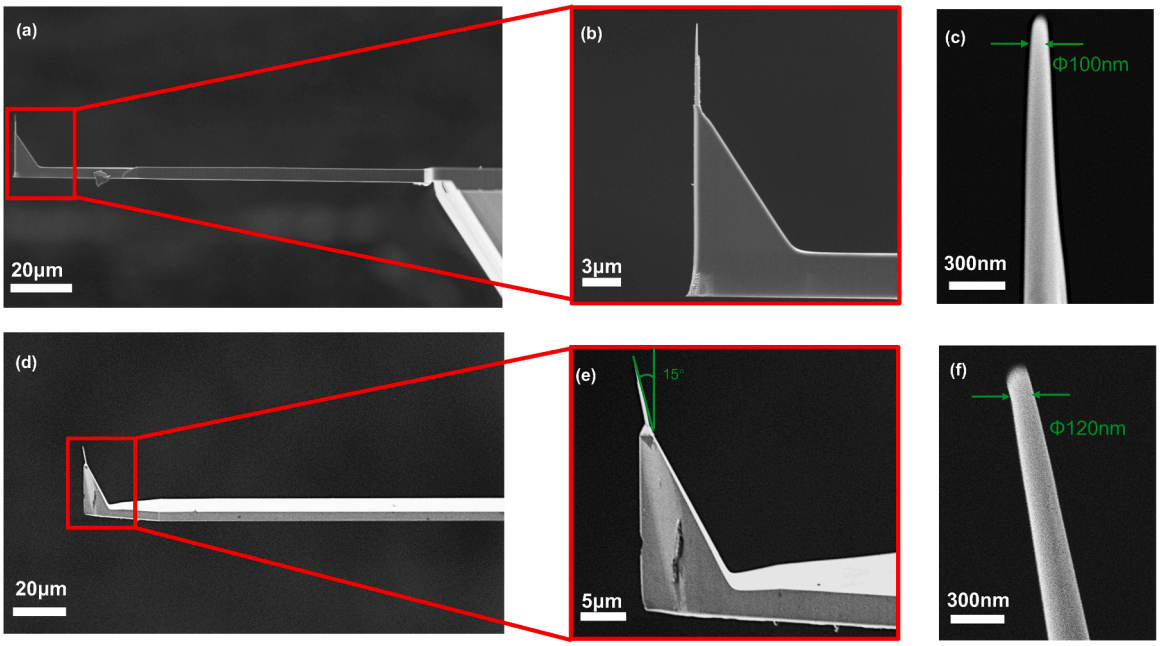

Fig. 3. The HAR nanopillar was sharpened and polished with a low ion beam current (30 kV, 1pA), resulting in a probe with a diameter of 100 nm and a height of about 10 μm, which is positioned at the top of a tip with a tilting angle of 0° ((a)-(c)) and 15° ((d)-(f)) respectively.

capability of the shape control. This indicates that nanopillars with diverse shapes, such as spirals, can be achieved using FIB deposition.

To improve the scanning resolution of the HAR probes, ion beam etching was used to sharpen the deposited Pt nanopillar. Fig. 3 presents two sharpened HAR probes with different tilting angles. Fig. 3(a) illustrates the HAR probe with a Pt tip with a height of about 10 μm, which was positioned at the top of a tip angle of 0°. As shown in Fig. 3(b), the upper diameter part of the tip was sharpened by ion beam etching. The upper diameter part of the tip can be identified in Fig. 3(c), which was less than 100 nm and can be used to improve scanning resolution. To demonstrate the effect of the angle of the HAR probe tip on the true morphology of the scanned 3-D samples, we fabricated an HAR probe tip with a height of about 10 μm, deposited at the top of a tip with a tilting angle of 15°. Fig. 3(d) and Fig. 3(e) present the HAR probe tip with the tilting angle 15° sharpened nanopillar. The upper diameter part of the probe tip can be identified in Fig. 3(f), which was less than 120 nm. These two probes were compared in the performance of scanning in the following section.

3.1. Application (1): Topography scanning

To verify the superiorit of HAR probes over commercial pyramid-shaped probes in scanning HAR structures, we performed AFM topography measurements on silicon trenches produced by FIB etching.

These trenches are HAR structures with depths ranging from 600 nm to 2.2 μm and a width of 1.5 μm as shown in Fig. 4(d).

Fig. 4(a)-(c) show schematic diagrams of HAR probes with a 15° tilting tip, a 0° tilting tip, and a commercial pyramid-shaped tip as well as topography measurements obtained by these three probes. The 3-D results plotted in Fig. 4(a)(b) precisely illustrate the true depth of the trench at a depth of 2 μm. However, the AFM probe with the pyramid-shaped tip could not reach the bottom of the deep trench and the obtained topography image could not reflect the depth of the HAR trench. The depth of the trenches scanned by the AFM probe with the pyramid-shaped tip was only about 400 nm (Fig. 4(c)), much lower than the true depth shown by the SEM image (Fig. 4(d)).

Fig. 4(e) summarized the true trench depths measured in the SEM diagram and measured by the three different AFM probes. The depth of the trenches measured by the HAR probe tip with 15° tilting angled is extremely close to the depth obtained by the SEM diagram, while the depth measured by the pyramid-shaped commercial probe in all five trenches was about 400 nm, which did not reflect the true depths of the trenches at all. This work demonstrates that the HAR probe can provide a more reliable and correct measurement of HAR trenches, and the superiority of the HAR probe is presented. Nevertheless, the HAR probe tip with a tilting angle of 0° still cannot completely reflect the true topography of the bottom of the HAR trench (Fig. 4(f)). Fig. 4(a), 4(b), and 4(f) compared the profiles of the HAR trench measured by HAR probe tip with a tilting angle of 15° to that of a tilting angle of 0°. It can be observed that the bottom width measured by the HAR probe tip with a tilting angle of 0° is narrower than the width measured by the HAR probe tip with a tilting angle of 15°, which is closer to the true topography. The probe tip of tilting angle of 15° can more accurately describe the bottom morphology of the HAR trench.

3.2. Application (2): Surface tension measurement

The HAR probe can be used not only for obtaining accurate topography of HAR structures but also for measuring the surface tension of a single micro/nanometer-scale liquid droplet[20,43]. Few studies

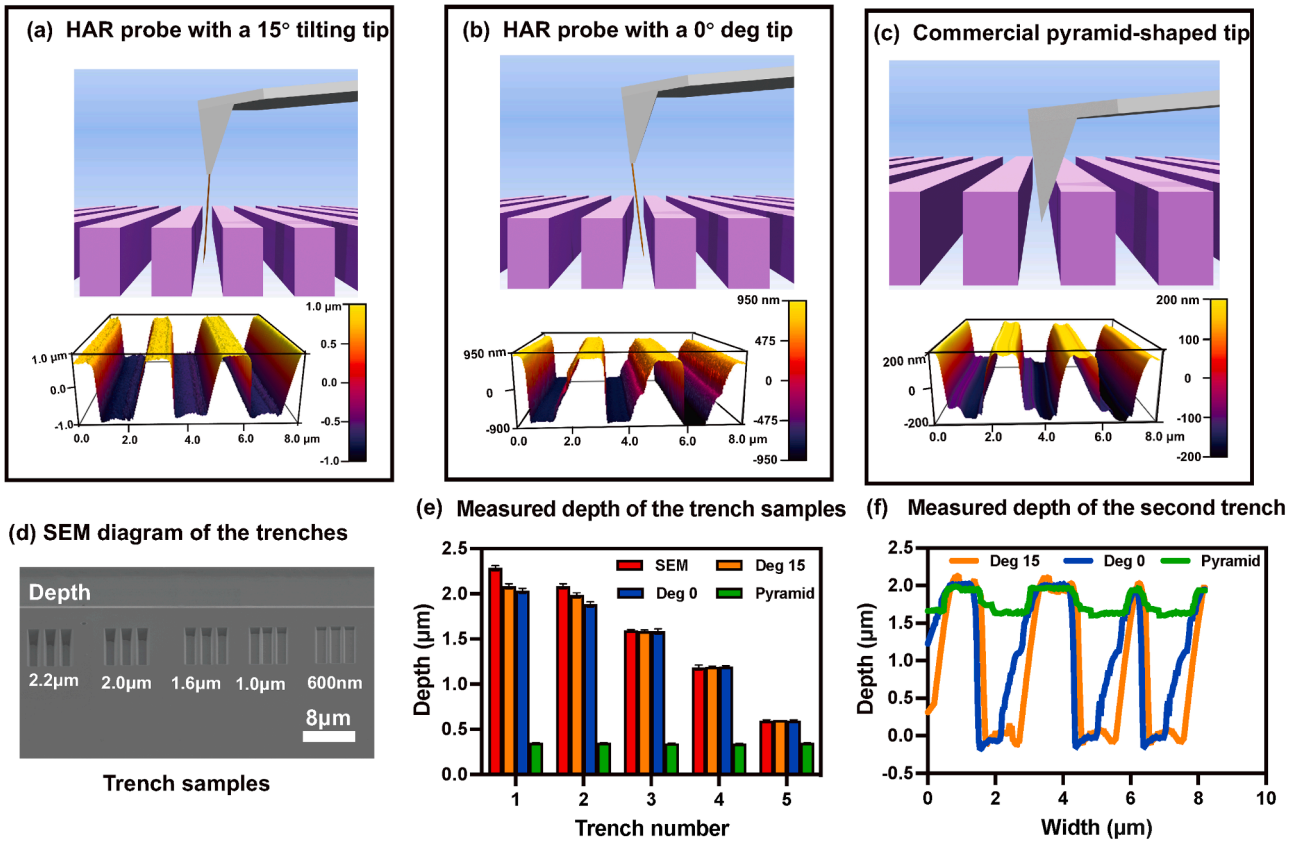

Fig. 4. (a)-(c) presents schematic diagrams of an HAR probe tip with a tilting angle of 15°, an HAR probe tip with a tilting angle of 0°, and a commercial pyramid-shaped probe when scanning an HAR trench, and their respective scanned 3D result graphs. (d) The SEM diagram of the HAR trench. (e) The measured trench depths by the SEM diagram, by the HAR AFM probes with different tilting angles and by the commercial pyramid-shaped probes. (f) The curve of the depths of the second HAR trench measured by the HAR probe tips with different tilting angles and the commercial pyramid-shaped probes.

applied this method, possibly due to the difficulty of fabricating AFM probes with HAR tips. It is an excellent application to use the HAR probe to measure the surface tension of a single micro/nanodroplet. The theory of surface tension calculation is based on the force curve of AFM probe extension into and retraction from the micro/nanodroplet. The AFM probe need to have an HAR tip of a constant diameter. The surface tension of the micro/nanodroplet is calculated through the formula (1),

$$F_{Ret} = 2\pi\sigma r \quad (1)$$

where r is the radius of the HAR tip indicated by the SEM image, F_{Ret} is the retention force in the measured force curve, and the surface tension σ of the micro/nanodroplets can be calculated. F_{Ret} is the force measured when the HAR tip breaks away from the surface of a droplet [20] (Fig. 5). The radius r of the HAR probe must be constant to obtain the surface tension of the micro/nanodroplet according to the Formula (1).

Fig. 5 shows the procedures of surface tension measurement. There are several experimental methods available that can measure the surface tension of bulk liquid systems, such as the Du Noüy tensiometer and Wilhelmy plate technique. The principle of these techniques is to use the retraction force of a metal ring, a metal disc, or a cylindrical wire that has been extended into the liquid surface and then retracted out. Fig. 5 (a) illustrates a schematic diagram of a conventional force tensiometer, the diameter of the tensiometer micro-needle is about 0.5 mm. Nevertheless, this experimental technique cannot provide measurement of surface tension on micro/nanometer scale droplets, since the size of the needle tip of a conventional force tensiometer is larger than the micro/nanometer scale droplets. Therefore, as shown in Fig. 5(b), an HAR AFM probe with a constant diameter of hundreds of nanometers can be employed to measure the surface tension of micro/nanodroplets. Fig. 5 (c) illustrates the different stages of surface tension measurement of micro/nanometer scale droplets using an HAR probe. The force at point A is that the tip of the HAR probe has not touched a single micro/nanodroplet, so the micro-cantilever is not bent. At point B, the tip of the HAR probe just starts to touch a single micro/nanometer scale droplet and the micro-cantilever is subject to a tiny attraction force. As the micro-cantilever continues drop down to point C, the tip is attracted by a greater attraction force, because when the tip contacts with the liquid, a spontaneously formed meniscus rises on the tip, bending the probe downward, resulting in the increased attraction force. At point C, we keep the HAR probe in position for a set dwell time (2 s) to provide stable measurement. At point D, the probe is quickly withdrawn from the droplet and the probe experiences a maximum attraction force when the tip leaves the liquid interface. In the end, the probe leaves the droplet and reaches point E. The force exerted on the probe during the withdrawal from point D to point E is the retention force in Formula (1).

The HAR probe in this experiment was fabricated based on the commercial probe Multi75Al-G (BudgetSensors) by the ion beam induced deposition of FIB and had a constant diameter of 322 nm as shown in Fig. 6(c). There were scattered white dots around the tip in Fig. 6(c), which were Pt deposited due to reaction of auxiliary gas containing Pt compounds and high-energy Ga ion beams. The size of the dots was small, thus they did not influence surface tension measurements. Liquid micro/nanodroplets of inorganic ultrapure water and organic 1,3-propylene glycol, whose surface tensions are previously reported in the literature [44,45], are selected for the surface force measurement using HAR probes. The droplet of around 3 μL was dripped on a hydrophobic silicon wafer [46] for surface tension testing by the HAR probe using AFM.

Examples of force plots for water and 1,3- propylene glycol are shown in Fig. 7. The measured retention force (F_{Ret}) for pure water is 72.1 nN ± 1.8 nN, which is an average of 10 tests, and surface tension is calculated to be 71.2 mN/m ± 1.8 mN/m. Similarly, the measured retention force for pure 1,3- propylene glycol is 45.4 nN ± 0.7 nN, which is an average of 20 tests, and surface tension is calculated to be 44.8 mN/m ± 0.7 mN/m. The acquired surface tension is similar to that reported in the literature, which are 72.0 mN/m for water and 45.8 mN/m for 1,3- propylene glycol, respectively [44,47]. Based on this established method of surface tension measurement for micro/nanodroplets, further measurements of surface tension of collected atmospheric particulate matters will be conducted and will be published in the future.

3.3. Robustness of HAR probe

To verify the robustness of the probe for this fabrication method, experiments relevant to the performance of the probe robust were conducted. The first experiment was to scan the high aspect ratio trench using the high aspect ratio probe at different scanning speeds, each scanning speed was repeated 25 times, and the SEM plots of the probe before and after scanning are presented below. The second experiment was to measure the surface tension of 1-propanol by changing the dwell time between the HAR probe approaching and retracting from the droplet. One hundred times force curves for each test were acquired.

The probe SEM plots before and after the force curve measurement

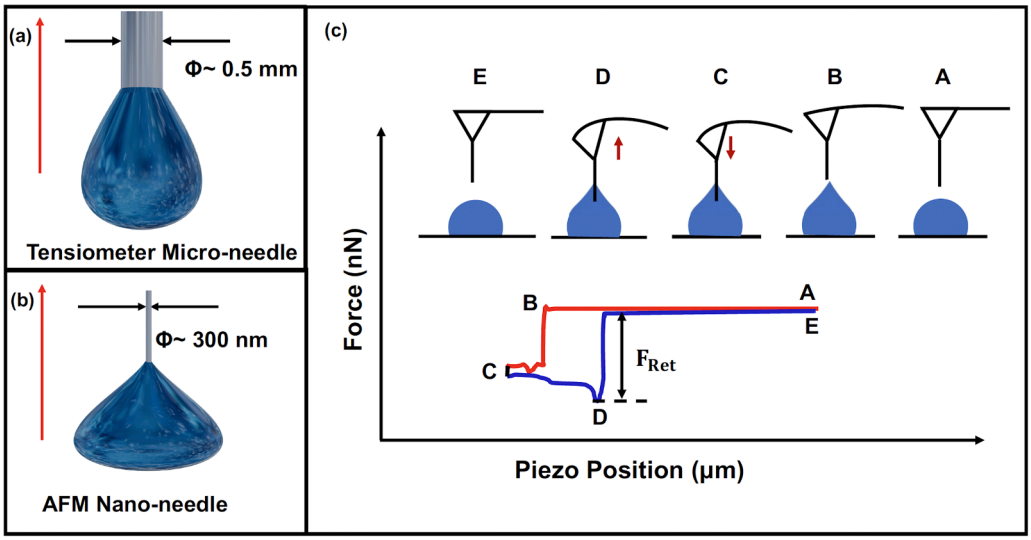

Fig. 5. (a) A schematic diagram of a conventional force tensiometer. (b) A schematic diagram of AFM nano-needle. (c) Typical AFM force plot measurement depicts the series of events that occur during the approach (red) and retract (blue) cycle of the AFM cantilever on the micro/nanodroplet. The retention force (F_{Ret}) is used to quantify the surface tension.

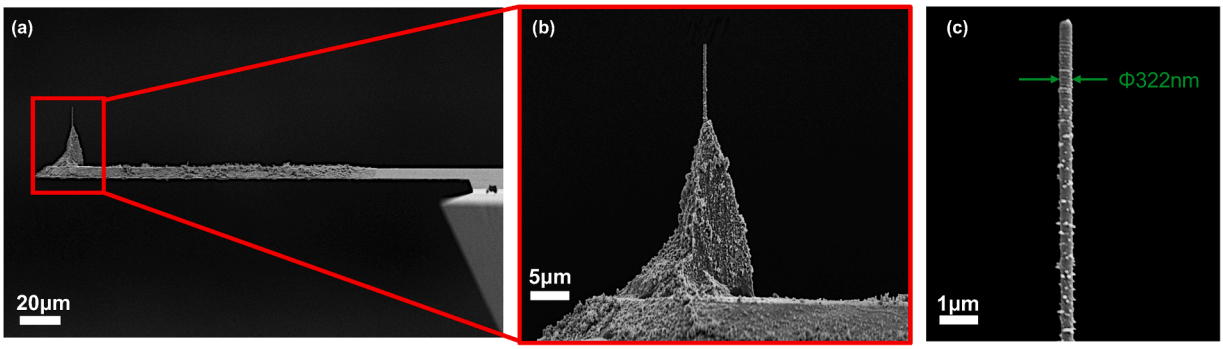

Fig. 6. (a)-(c) The HAR nanopillar was controlled by constant diameter, resulting in a probe with a diameter of 322 nm and a height of about 11 μm.

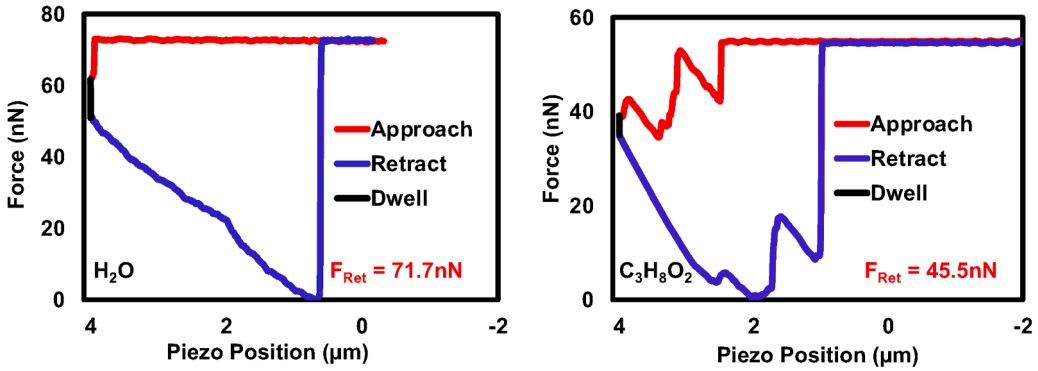

Fig. 7. Surface tension test results of micro/nanodroplets of two samples, (a) the surface tension test result of pure water, (b) the surface tension test result of 1,3-propylene glycol.

are presented below. As can be observed from Fig. 8, there is no change in the probe before and after scanning at different speeds. The height morphology of the test is plotted and is highly reproducible. As can be observed from Fig. 9, there is no change in the probe before and after 400 force profiles were acquired setting different dwell times. From the above two experiments, it can be found that the high aspect ratio probes fabricated by this method can satisfy the functions of scanning morphology and testing surface tension. Besides, it could maintain good repeatability of the results when changing different parameters. Fig. 8 illustrates that the depth of the scanned topography reaches the actual depth and topography when scanning HAR trenches. Fig. 9 illustrates the surface tension of 1-propanol obtained from different dwell time

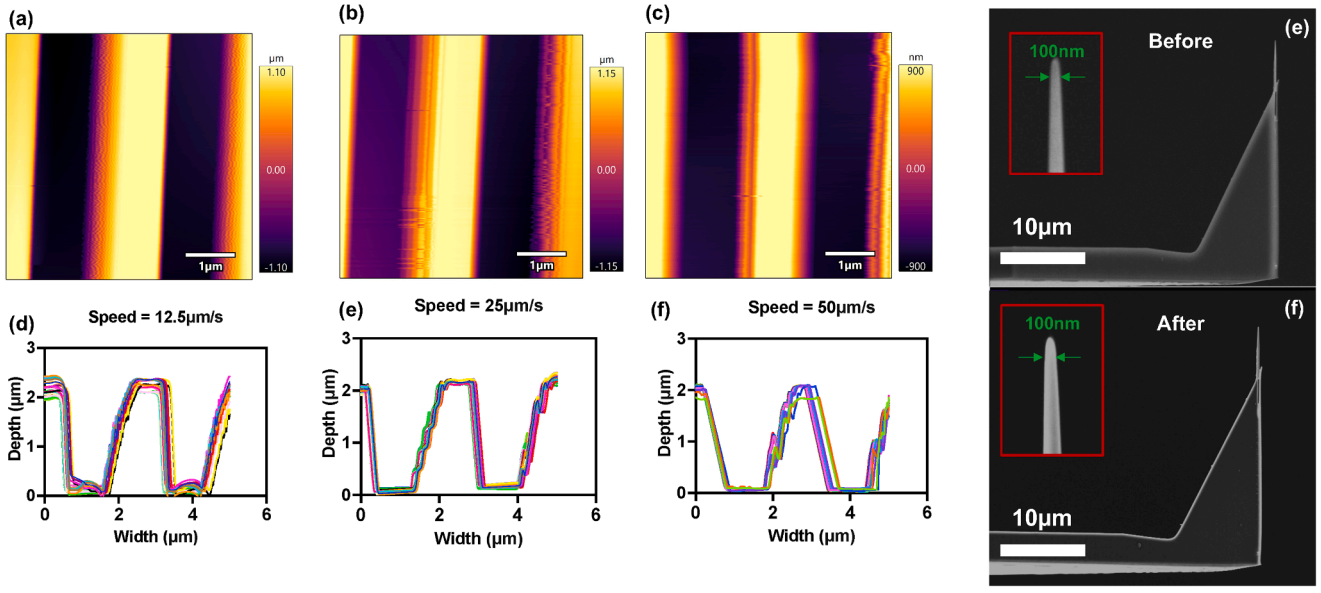

Fig. 8. Scanning the high aspect ratio trench using the high aspect ratio probe at different scanning speeds. Figures (a-c) illustrate the scanning speed of 12.5 μm/s, 25 μm/s and 50 μm/s to scan high aspect ratio trenches, respectively. Figures (d-f) show the height profiles of 25 repetitions of different scanning speeds. Figures (g) and (h) present the SEM plots of the high aspect ratio probe before and after scanning. There is almost no change in the probe before and after scanning the sample at different speeds.

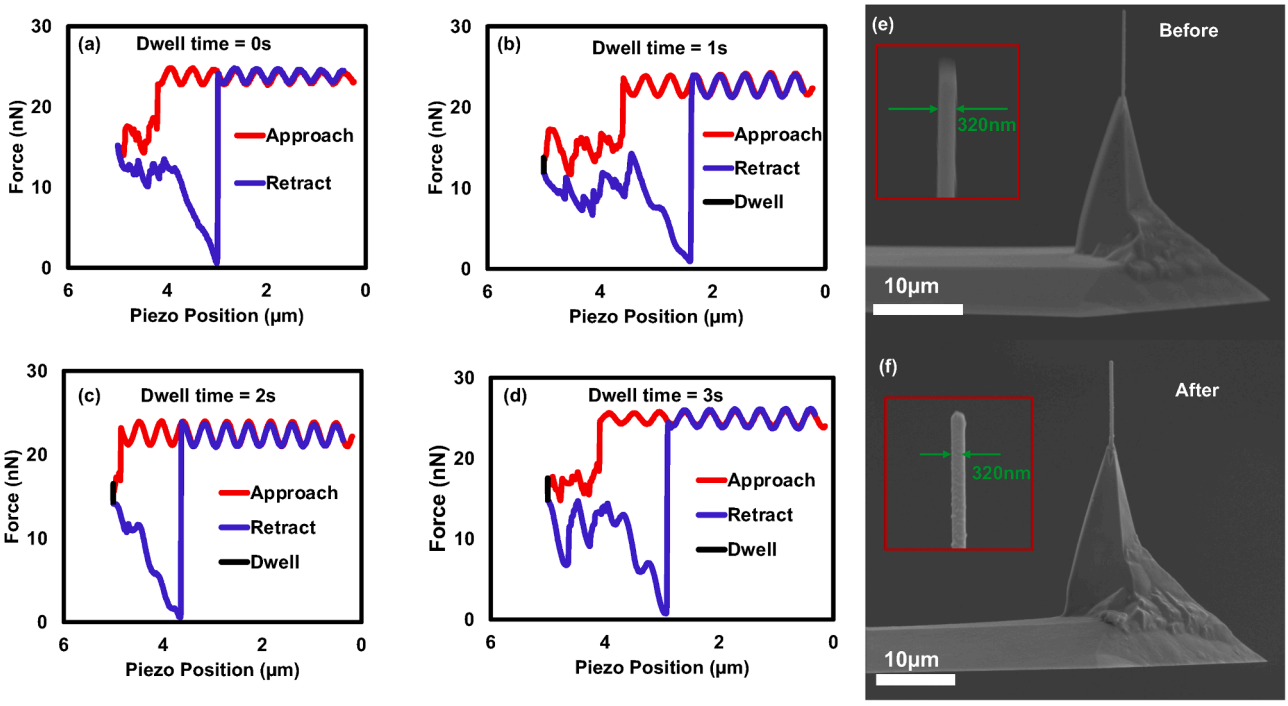

Fig. 9. The surface tension of 1-propanol was measured at different dwell times using our fabricated high aspect ratio probe. Figures (a-d) present the surface tension of 1-propanol measured for dwell times of 0–3 s, respectively. Figures (e) and (f) present the SEM plots before and after the high aspect ratio probe force curve measurement. There is almost no change in the HAR probe before and after force curve measurement at different dwell times.

tests calculated from Eq. 1 is 23.2 mN/m ± 0.4 mN/m, 23.3 mN/m ± 0.2 mN/m, 23.3 mN/m ± 0.2 mN/m, 23.2 mN/m ± 0.3 mN/m, respectively, which are consistent with the theoretical value 23.34 mN/m [48]. Therefore, it can be concluded that the probe fabricated by this method was robust.

We have demonstrated a method to fabricate HAR AFM probes for AFM utilizing the etching and deposition capabilities of FIB. The most important advantage of this method is that the diameter, the height, and the tilting angle of the HAR tip can be precisely controlled within a certain range, which can enable precise measurements for high aspect ratio structures and accurate measurements for surface tension in micro/nanometer scale droplets. The fabricated probes are extremely reproducible and can be used in a variety of applications, including mechanical properties of atmospheric particulate matters, e.g., viscosity, which influences the chemical reaction of particles and gaseous species and further impacts air pollution and climate [49]. Nevertheless, the minimum diameter achieved by this method is relatively large compared to the minimum diameter of commercial pyramid-shaped probes. The limitations of using FIB to fabricate probes include: the suitable materials are limited to such as Pt and C, and the cost of FIB is relatively high, and ion beam etching to optimize the diameter is limited by the minimum beam current of 1pA in the instrument. As seen in the video in the supporting material, when the ion beam continuously optimized the diameter, the diameter did not reduce all the time but reached a limit when it became smaller to a certain diameter (about 80 nm). If it continued to be etched, the optimized part disappeared, and so on. It may be because the beam spotsize of the minimum processed ion beam current is around 25 nm [50]. Thus, it is still a challenge to fabricate a HAR tip with a sub-50 nm diameter.

4. Conclusions

This paper has demonstrated a method to fabricate HAR probes that can control the diameter, the height, and the tilting angle of HAR probes within a certain range. A maximum aspect ratio of 40, a maximum height of 20 μm, a minimum diameter of 100 nm, and a tip of 15° tilting angle were achieved.

Two types of tests were selected to test the performance of the fabricated HAR probes. One was to test the accuracy of scanning topography by HAR probes. Scanning the topography of HAR nanotrenches, the fabricated HAR probes could acquire the vertical sidewall topography and depth of HAR trenches well, while commercial pyramid probes could not reflect the true topography of HAR trenches. It reflects the superiority of HAR probes in scanning such structures. The second was to test the force curves of the micro/nanodroplets utilizing the constant-diameter HAR probe. The surface tension values of micro/nanodroplets of inorganic pure water and organic 1,3-propylene glycol micro/nanodroplets were obtained by this method accurately and efficiently.

CRediT authorship contribution statement

Xiaolei Ding: Methodology, Formal analysis, Writing – review & editing. **Binyu Kuang:** Methodology, Writing – review & editing. **Chun Xiong:** Investigation. **Renwei Mao:** Investigation. **Yang Xu:** Investigation. **Zhibin Wang:** Resources. **Huan Hu:** Resources, Supervision.

Declaration of Competing Interest

The authors declare that they have no known competing financial interests or personal relationships that could have appeared to influence the work reported in this paper.

Data Availability

Data will be made available on request.

Acknowledgements

This work was partly supported by ZJUI and led by Prof. Huan Hu. This work was also financially supported by the National Natural Science Foundation of China (Grant No. 61974128, 91844301, 42005087),

the Center of Pathogen Detection in the Dynamic Research Enterprise for Multidisciplinary Engineering Sciences (DREMES), and Cyrus Tang Foundation. We thank the Nano Laboratory of Zhejiang University International Campus for providing focused ion beam instrument (ZEISS Crossbeam 350). We thank Professor Shikuan Yang at Zhejiang University for providing hydrophobic silicon wafers.

Appendix A. Supporting information

Supplementary data associated with this article can be found in the online version at doi:10.1016/j.sna.2022.113891.

References

[1] J.-H. Ahn, J.H. Je, Stretchable electronics: materials, architectures and integrations, J. Phys. D: Appl. Phys. 45 (10) (2012), 103001.
[2] J. Lee, et al., A light-driven supramolecular nanowire actuator, Nanoscale 7 (15) (2015) 6457–6461.
[3] Y.-L. Zhang, et al., Designable 3D nanofabrication by femtosecond laser direct writing, Nano Today 5 (5) (2010) 435–448.
[4] C.-C. Liu, et al., Directed self-assembly of block copolymers for 7 nanometre FinFET technology and beyond, Nat. Electron. 1 (10) (2018) 562–569.
[5] G. Vereecke, et al., Wet etching of TiN in 1-D and 2-D confined nano-spaces of FinFET transistors, Microelectron. Eng. 200 (2018) 56–61.
[6] X. Tang, et al., A simple method for measuring Si-Fin sidewall roughness by AFM, IEEE Trans. Nanotechnol. 8 (5) (2009) 611–616.
[7] A.T. Woolley, et al., Structural biology with carbon nanotube AFM probes, Chem. Biol. 7 (11) (2000) R193–R204.
[8] J. Bunch, T. Rhodin, P. McEuen, Noncontact-AFM imaging of molecular surfaces using single-wall carbon nanotube technology, Nanotechnology 15 (2) (2004) S76.
[9] N.R. Wilson, J.V. Macpherson, Carbon nanotube tips for atomic force microscopy, Nat. Nanotechnol. 4 (8) (2009) 483–491.
[10] F. Priolo, et al., Silicon nanostructures for photonics and photovoltaics, Nat. Nanotechnol. 9 (1) (2014) 19–32.
[11] Y. Ma, et al., Processing study of SU-8 pillar profiles with high aspect ratio by electron-beam lithography, Microelectron. Eng. 149 (2016) 141–144.
[12] Y. Ma, et al., A simple method for fabrication of high-aspect-ratio all-silicon grooves, Appl. Surf. Sci. 284 (2013) 372–378.
[13] Y. Zhuo, et al., Photonic crystal slab biosensors fabricated with helium ion lithography (HIL), Sens. Actuators A: Phys. (2019) **297**.
[14] N.L. Privorotskaya, et al., Sensing micrometer-scale deformations via stretching of a photonic crystal, Sens. Actuators A: Phys. 161 (1–2) (2010) 66–71.
[15] B. Wu, A. Kumar, S. Pamarthy, High aspect ratio silicon etch: a review, J. Appl. Phys. 108 (5) (2010) 9.
[16] H. Köhler, *The nucleus in and the growth of hygroscopic droplets*, Trans. Faraday Soc. 32 (1936) 1152–1161.
[17] J.H. Seinfeld, et al., Improving our fundamental understanding of the role of aerosol– cloud interactions in the climate system, Proc. Natl. Acad. Sci. 113 (21) (2016) 5781–5790.
[18] A.M.K. Hansen, et al., Hygroscopic properties and cloud condensation nuclei activation of limonene-derived organosulfates and their mixtures with ammonium sulfate, Atmos. Chem. Phys. 15 (24) (2015) 14071–14089.
[19] K. Lunkenheimer, K.-D. Wantke, Determination of the surface tension of surfactant solutions applying the method of Lecomte du Noüy (ring tensiometer), Colloid Polym. Sci. 259 (3) (1981) 354–366.
[20] H.D. Lee, et al., Direct surface tension measurements of individual sub-micrometer particles using atomic force microscopy, J. Phys. Chem. A 121 (43) (2017) 8296–8305.
[21] J.H. Hafner, et al., Structural and functional imaging with carbon nanotube AFM probes, Prog. Biophys. Mol. Biol. 77 (1) (2001) 73–110.
[22] H.W. Lee, et al., The effect of the shape of a tip's apex on the fabrication of an AFM tip with an attached single carbon nanotube, Sens. Actuators A: Phys. 125 (1) (2005) 41–49.
[23] M. Behzadirad, et al., GaN nanowire tips for nanoscale atomic force microscopy, Nanotechnology 28 (20) (2017) 20LT01.
[24] K. Mølhave, et al., Pick-and-place nanomanipulation using microfabricated grippers, Nanotechnology 17 (10) (2006) 2434.
[25] K. Carlson, et al., A carbon nanofibre scanning probe assembled using an electrothermal microgripper, Nanotechnology 18 (34) (2007), 345501.
[26] S.C. Tan, H. Zhao, C.V. Thompson, Fabrication of high aspect ratio AFM probes with different materials inspired by TEM "lift-out" method, J. Vac. Sci. Technol. B, Nanotechnol. Microelectron.: Mater. Process. Meas. Phenom. 34 (5) (2016), 051805.
[27] J. Li, A.M. Cassell, H. Dai, Carbon nanotubes as AFM tips: measuring DNA molecules at the liquid/solid interface, Surf. Interface Anal.: Int. J. devoted Dev. Appl. Tech. Anal. Surf., Interfaces thin films 28 (1) (1999) 8–11.
[28] D.S. Engstrom, et al., High throughput nanofabrication of silicon nanowire and carbon nanotube tips on AFM probes by stencil-deposited catalysts, Nano Lett. 11 (4) (2011) 1568–1574.
[29] P. Knittel, et al., Focused ion beam-assisted fabrication of soft high-aspect ratio silicon nanowire atomic force microscopy probes, Ultramicroscopy 179 (2017) 24–32.
[30] B.A. Bryce, et al., Silicon nanowire atomic force microscopy probes for high aspect ratio geometries, Appl. Phys. Lett. 100 (21) (2012), 213106.
[31] J. Brown, et al., Electrically conducting, ultra-sharp, high aspect-ratio probes for AFM fabricated by electron-beam-induced deposition of platinum, Ultramicroscopy 133 (2013) 62–66.
[32] A. Savenko, et al., Ultra-high aspect ratio replaceable AFM tips using deformation-suppressed focused ion beam milling, Nanotechnology 24 (46) (2013), 465701.
[33] O. Ageev, et al., Fabrication of advanced probes for atomic force microscopy using focused ion beam, Microelectron. Reliab. 55 (9–10) (2015) 2131–2134.
[34] J. Skibinski, et al., Imaging resolution of AFM with probes modified with FIB, Micron 66 (2014) 23–30.
[35] M. Wendel, H. Lorenz, J. Kotthaus, Sharpened electron beam deposited tips for high resolution atomic force microscope lithography and imaging, Appl. Phys. Lett. 67 (25) (1995) 3732–3734.
[36] M.M. Yazdanpanah, et al., Selective self-assembly at room temperature of individual freestanding Ag 2 Ga alloy nanoneedles, J. Appl. Phys. 98 (7) (2005), 073510.
[37] R. Jalilian, et al., Toward wafer-scale patterning of freestanding intermetallic nanowires, Nanotechnology 22 (29) (2011), 295601.
[38] N.R. Wood, et al., Dielectrophoretic trapping of nanoparticles with an electrokinetic nanoprobe, Electrophoresis 34 (13) (2013) 1922–1930.
[39] F.S. Jamaludin, M.F. Mohd Sabri, S.M. Said, Controlling parameters of focused ion beam (FIB) on high aspect ratio micro holes milling, Microsyst. Technol. 19 (12) (2013) 1873–1888.
[40] Y. Li, et al., An experiment-based method for focused ion beam milling profile calculation and process design, Sens. Actuators A: Phys. 286 (2019) 78–90.
[41] J. Melngailis, Focused ion beam technology and applications, J. Vac. Sci. Technol. B: Microelectron. Process. Phenom. 5 (2) (1987) 469–495.
[42] R.J. Cannara, M.J. Brukman, R.W. Carpick, Cantilever tilt compensation for variable-load atomic force microscopy, Rev. Sci. Instrum. 76 (5) (2005), 053706.
[43] J. Baltrusaitis, V.H. Grassian, *Atomic force microscopy and X-ray photoelectron spectroscopy study of NO2 reactions on CaCO3 (1014) surfaces in humid environments*, J. Phys. Chem. A 116 (36) (2012) 9001–9009.
[44] C.M. Romero, M.S. Paéz, Surface tension of aqueous solutions of alcohol and polyols at 298.15 K, Phys. Chem. Liq. 44 (1) (2006) 61–65.
[45] N. Pallas, Y. Harrison, An automated drop shape apparatus and the surface tension of pure water, Colloids Surf. 43 (2) (1990) 169–194.
[46] Q. Ding, et al., Quantitative and sensitive SERS platform with analyte enrichment and filtration function, Nano Lett. 20 (10) (2020) 7304–7312.
[47] N. Vargaftik, B. Volkov, L. Voljak, International tables of the surface tension of water, J. Phys. Chem. Ref. Data 12 (3) (1983) 817–820.
[48] J.J. Jasper, The surface tension of pure liquid compounds, J. Phys. Chem. Ref. Data 1 (4) (1972) 841–1010.
[49] H.D. Lee, K.K. Ray, A.V. Tivanski, Solid, semisolid, and liquid phase states of individual submicrometer particles directly probed using atomic force microscopy, Anal. Chem. 89 (23) (2017) 12720–12726.
[50] N. Smith, et al., High brightness inductively coupled plasma source for high current focused ion beam applications, J. Vac. Sci. Technol. B: Microelectron. Nanometer Struct. Process. Meas. Phenom. 24 (6) (2006) 2902–2906.

Miss. Xiaolei Ding is a doctoral student jointly trained by the School of Micro and Nano Electronics of Zhejiang University and Zhejiang University-University of Illinois at Urbana-Champaign Institute (ZJUI). She is currently working on the fabrication of a wide variety of AFM probes and the study of surface physical properties of 2D materials.

Dr. Binyu Kuang is a postdoc in College of Environmental and Resource Sciences, Zhejiang University. He is currently working on factors influencing cloud condensation nuclei activity of atmospheric particulate matters, and source apportionment of particulate matters. He has published 3 SCI papers.

Mr. Chun Xiong is a Ph.D. student in College of Environmental and Resource Sciences, Zhejiang University. He is currently working on cloud condensation nuclei activity of atmospheric particulate matters, such as surface tension measurement of particulate matters.

Dr. Renwei Mao is currently a postdoctoral researcher at Zhejiang University-University of Illinois at Urbana-Champaign Institute. His research is in flexible electronics. He is familiar with micro-nano manufacture technology including UV Lithography, SEM, E-beam evaporation, ICP etching and other electrical testing equipment. He has published 3 SCI papers so far.

Prof. Yang Xu is an IEEE Distinguished Lecturer, Professor of ZJU-UIUC Joint Institute, Professor of School of Micro and Nano Electronics, Professor of School of Information and Electronic Engineering, and Professor of ZJU-UIUC Joint Institute. His current research interests are focused on emerging smart sensors and imagers for the Internet-of-Everything/Intelligence (IoE/IoI) and Ubiquitous Electronics. He has published more than 120 SCI journal papers including Nature Electronics, Nature Nanotechnology, Nature Photonics, Chem. Rev., Nature Comm, Adv. Mater. , Phys. Rep., Chem. Soc. Rev., Nano Lett., ACS Nano, Phys. Rev. Lett. and IEDM, with citations over 4500 times, and an H-index of 37. He holds 30 granted patents and gave more than 60 invited talks in MRS, ACS, APS, CPS, OSA, AIP, IOP, IEEE and Nature conferences. He is IEEE distinguished lecturer and also served as Associate Editor of IEEE Nanotechnology Magazine.

Prof. Zhibin Wang is a researcher in College of Environmental and Resource Sciences, Zhejiang University. He is currently working on several aspects of atmospheric particulate matters, including new particle formation, hygroscopic growth, cloud condensation nuclei activity, optical properties, characteristics of secondary particulate matters, source apportionment of particulate matters, and also development of instruments of particulate matters measurements. He has led several projects in academia. He has published more than 10 SCI papers as first author or corresponding author so far.

Prof. Huan Hu is an assistant professor at Zhejiang University-University of Illinois at Urbana-Champaign Institute (ZJUI) and vice minister of the Education Department of Zhejiang University International Campus. His research interest includes advanced nanomanufacturing, bio-inspired sensing, micro/nano-sensors, and lab on a chip. He is now leading the Nanomanufacturing and Biomimetics Research Group at ZJUI. His research focuses on nanotechnology, digital fabrication, and experiments on chips and advanced sensors. He has led projects in both academia and industry, resulting in the publication of 16 peer-reviewed journal articles and 14 published patents. In addition, he has assisted and led several successful grant programs.